Comparative study on the water uptake kinetics and dehumidification performance of silica gel and aluminophosphate zeolites coatings

*Author names and affiliations:

Lin Liu,[a, c] Mitsuhiro Kubota,*[b] Jun Li,*[a, c] Hayato Kimura,[b] Yu Bai,[a,c] Rongjun Wu,[b] Lisheng Deng,[a,c,d] Hongyu Huang,[a, c] Noriyuki Kobayashi[b]

[a] *Guangzhou Institute of Energy Conversion, Chinese Academy of Sciences, 510640, No.2, Nengyuan Rd., Wushan, Tianhe District, Guangzhou, P. R. China*

[b] *Department of Chemical Systems Engineering, Graduate School of Engineering, Nagoya University, 464-8603, Furo-cho, Chikusa-ku, Nagoya-shi, Aichi, Japan*

[c] *Southern Marine Science and Engineering Guangdong Laboratory (Guangzhou), 511458, No.1119, Haibin Rd., Nansha District, Guangzhou, P. R. China*

[d] *Guangdong Intelligent Filling Technology Limited Company, 528137, No.63 (F3)-5, Zone C, Sanshui Industrial Park, Foshan, Guangdong, P. R. China*

* To whom correspondence should be addressed

Corresponding author:

Mitsuhiro Kubota

E-mail: kubota.mitsuhiro@material.nagoya-u.ac.jp

Tel/Fax numbers: +81 52-789-5597/+81 52-789-3842

Nagoya University, Furo-cho, Chikusa-ku, Nagoya-shi, Aichi 464-8603, Japan

Jun Li

E-mail: lijun@ms.giec.ac.cn

Tel/Fax numbers: +86 20-37210762/+86 20-87013240

Guangzhou Institute of Energy Conversion, Chinese Academy of Sciences, No. 2 Nengyuan Rd, Wushan, Tianhe District, Guangzhou 510640, P. R. China

Abstract

Desiccant coated heat exchanger (DCHE) systems have significant potential in improving dehumidification performance. The moisture transfer occurring in one single air channel of DCHE can dominate the overall system performance. In this study, the adsorber with an approximate air channel of DCHE was designed to experimentally investigate the kinetics of silica gel and two aluminophosphate zeolites (FAM Z01 and FAM Z05). Their dehumidification performances also were simulated at regeneration temperature range of 50-80℃ to reveal the applicability in air-cooled cross-flow DCHE. Results showed that linear driving force (LDF) model could well describe the dynamic water uptake behaviors. Adsorption rate coefficient k_{ads} increased with increasing inlet air humidity ratio and velocity, but decreased with increasing coating thickness. It is worth noting that increasing regeneration temperature had a little effect on k_{ads}, while desorption rate coefficient k_{des} increased significantly. Simulation results showed that moisture removal capacity (MRC) and dehumidification performance of coefficient (DCOP) of FAM Z05 coated DCHE could reach 0.495 g/kg and 0.57 at regeneration temperature of 50℃, which were 2.3 and 15.4 times higher than these of silica gel and FAM Z01 coated DCHEs. It demonstrated that FAM Z05 was more promising to utilize lower-grade heat energy.

Highlights

- Water uptake kinetics of silica gel, FAM Z01 and FAM Z05 coated adsorber were experimentally revealed.
- Dehumidification performances of three desiccant types DCHEs were numerically compared.
- LDF model could well describe the kinetics of three desiccants coated adsorber.
- FAM Z05 coated DCHE showed larger potential in utilizing lower-grade heat energy.

Keywords
Aluminophosphate zeolite; Adsorption kinetics; Dehumidification performance; Desiccant coated heat exchanger

Nomenclature		Δh_{vs}	vaporization latent heat of water (J)
A	sectional area (m^2)	*Greek symbols*	
C_{pa}	specific heat capacity (J/kg·K)	δ	thickness (m)
D	diffusion coefficient (m^2/s)	ρ	density (kg/m^3)
$DCOP$	dehumidification performance of coefficient	φ	relative humidity
k	rate coefficient (s^{-1})	*Subscript*	
$\dot{m}$	mass flowrate (kg/s)	0	initial
MRC	moisture removal capacity (kg/kg)	ads	adsorption
R^2	square of fitting correlation coefficient	des	desorption
R_g	water vapor gas constant	$duct$	air duct
t	time (s)	e	effective
u	velocity (m/s)	eq	equilibrium
$\dot{V}$	volume flowrate (m^3/s)	in	inlet
W	water uptake (kg/kg)	max	maximum
Y_a	humidity ratio (kg/kg)	out	outlet

1. Introduction

High thermal comfort and low energy consumption in buildings have recently become more desirable with the increasing demand of sustainable development strategies in the world. As one of the main parts of energy consumption of buildings, the refrigeration and air conditioning systems have accounted for 30% of total worldwide energy consumption [1]. In conventional refrigeration and air conditioning systems, the air first was supercooled below its dew point to condense out the moisture, and then the cold air was reheated to meet the temperature requirement of supply air. The coupling dealing of temperature and humidity with supercooling and reheating processes could result in an unsatisfactory thermal comfort and energy waste [2]. To reduce building energy consumption while providing a good thermal comfort, the development of independent control technologies of temperature and humidity could be therefore efficient solution [3-5]. As an effective candidate, solid dehumidification cooling systems can realize a less consumption of electricity and a utilization of low-grade thermal energy. As a result, they are considered as an attractive alternative for the conventional systems.

Solid dehumidification cooling systems can be classified into three types according to different constructions of dehumidifier: fixed bed, rotary bed and desiccant coated heat exchanger (DCHE) [6]. In both fixed bed and rotary bed, the moisture removal capacity could be decreased because of the released adsorption heat during adsorption process. The DCHE handling sensible and latent heat load simultaneously

was developed to address this drawback. Extensive research efforts have been made to obtain high-efficient DCHE systems by developing novel desiccant materials as well as optimizing structure of DCHE and system cycle [6-8].

Desiccant materials play an important role in developing DCHE systems due to the strong material dependence of overall performance of the systems [9, 10]. The high adsorption capacity and low regeneration temperature are generally preferred for dehumidification application. In past studies, silica gel has been widely employed in DCHEs, it can be regenerated at relative low temperature as well as has some advantages in stability and cost. However, its linear-shaped isotherm caused a slow adsorption rate and a possible small adsorption capacity especially at low regeneration temperature [11]. Research interests had been triggered in exploiting alternative desiccant materials with better adsorption performance even at lower regeneration temperature. A new generation of functional adsorbent material (FAM) zeolites developed by Mitsubishi Plastics Inc. became an effective choice in recent years. The FAM zeolites include three type aluminophosphate materials, i.e., FAM Z01, FAM Z02 and FAM Z05. The FAM Z01 and FAM Z05 are belonged to AFI type molecular sieves. They can be regenerated by the lower regeneration temperature compared to FAM Z02 due to their smaller adsorption capacity under low relative humidity range. Intensive researches on the utilization of FAM Z01 and FAM Z05 in the field of adsorption dehumidification and heat pump have been carried out [11-14]. Hong et al. [11] numerically compared the adsorption capacity of FAM Z01 and various type silica gels coated DCHEs. It demonstrated that FAM Z01 has a high potential to improve the performance and reduce system size. The dehumidification performances of FAM Z01 and FAM Z05 coated DCHEs also were evaluated by Shimooka et al. [15]. They found that FAM Z05 coated DCHE has better water adsorption capacity at lower regeneration temperature than FAM Z01. Zheng et al. [16] compared the dehumidification performance of FAM Z02, FAM Z05 and silica gel coated DCHEs based on a validated mathematical model. Results showed that FAM Z05 coated DCHE can have 2-3 times larger dehumidification capacity than these of FAM Z02 and silica gel especially at low regeneration temperature of 50-60℃. In our previous study [17], the dehumidification behavior of an air-cooled cross-flow DCHE coated with FAM Z01 was experimentally investigated. It was found that the dehumidified air could be supplied for practical use with a sufficiently low absolute humidity even at low regeneration temperature of 60℃.

Many studies have investigated the potential of FAM zeolites in improving the performance of DCHE systems under lower regeneration temperature. However, their adsorption kinetics in real or approximate air channel of DCHEs have not been revealed in detail, although they are very important for practical and large-scale applications of desiccant materials. In order to understand the kinetics of moisture transport in desiccant layer, the rigorous Fick's equation is generally required, but it is difficult to obtain the analytical solutions under practical situation [18]. By contrast, the well-known linear driving force (LDF) model provides a simple equation to correlate experimental data, which has been widely employed in investigating the adsorption kinetics of closed adsorption systems [19]. In several references [19-21], the LDF model also was proved to be able to well describe the dynamic behavior of open silica

gel coated DCHE systems. However, it should be noted that the applicability of LDF model is generally limited by the requirements of isothermal adsorption and enough adsorption time [18, 22]. In DCHEs, the desiccant coated on the surface of metal wall is well cooled by cold fluid at the cooling side of DCHEs during adsorption process, and the near-isothermal adsorption can be achieved except the initial stage of switching from regeneration to adsorption [20]. This fact supports the feasibility of the LDF model in predicting the water adsorption kinetics in open DCHE systems.

From the aforementioned findings, the comprehensive kinetics analysis of silica gel, FAM Z01 and FAM Z05 in approximate air channel of DCHEs are still lack. Moreover, although we investigated the dehumidification behaviors of silica gel and FAM Z01 coated air-cooled cross-flow DCHEs in the earlier studies [17, 23], seeking more suitable low-temperature regenerative desiccants for promoting the utilization of lower temperature heat sources is still the goal of further research work. Therefore, in this study, the comprehensive comparison of the three desiccants was carried out in terms of kinetics and dehumidification performance. The dynamic water uptake behavior of an adsorber with open parallel air channel coated with silica gel, FAM Z01 and FAM Z05 respectively were experimentally measured and fitted by LDF model under various parameters. A research effort was conducted to simulate the dehumidification performance of the three desiccant types air-cooled DCHEs with the same desiccant amount at regeneration temperature range of 50-80℃.

2. Experiment

2.1 Coating preparation

Materials used in this study mainly include RD silica gel, liquid binder, FAM Z01 and FAM Z05 slurries. The material properties were described in Table 1.

Table 1 Material properties

Name	Details	Manufacturer
RD silica gel	Particle size<7 μm	Fuji Silysia Chemical Co., Ltd.
FAM Z01 slurry	Mixture of FAM Z01 and binder	Mitsubishi Plastics Co., Ltd.
FAM Z05 slurry	Mixture of FAM Z05 and binder	Mitsubishi Plastics Co., Ltd.

Desiccant coated copper sheets were prepared by the following procedures: 1) The copper foil was cut into pieces with length 150 mm × width 100 mm and then fixed on a flat surface; 2) Three desiccant slurries were prepared. Silica gel and liquid binder with the mass ratio 9:1 were mixed with 50%wt deionized water. The mixture slurry was sonicated in an ultrasonic oscillator and continuously stirred for 5 minutes to disperse the desiccant particles. Similar procedures were used to prepare FAM Z01 and FAM Z05 slurries. Since the purchased FAM Z01 and FAM Z05 slurries already contained binder, only 25%wt and 35%wt deionized water were needed respectively in the preparation process; 3) A certain amount of slurry was taken to put on the copper sheet, and it was evenly coated by repeatedly pushing and pulling a steel mold with a gap at the bottom surface. Molds with various bottom gaps (The gap heights are 0.1 mm, 0.2 mm, 0.3 mm and 0.4 mm, respectively) were manufactured to prepare different thickness coatings. 4) Desiccant coated copper sheets were first dried in the atmosphere, and then cut into pieces with length 100 mm × width 20 mm. Here, considering the

deviation in cutting, the real size of each copper sheet was re-measured.

2.2 Thickness measurement

The thicknesses δ of desiccant coatings were measured using a surface roughness measuring instrument SV-3100 manufactured by Mitutoyo Company, Japan (Instrument resolution 10 nm). Since it was difficult to directly measure the thickness of coated desiccant on copper sheet, the desiccant coated copper plate prepared by the same procedures as the Section 2.1 was used as substitute. The prepared samples were first dried in the atmosphere, and then the thicknesses of five positions at the length direction of the desiccant coated plate were measured respectively, where the calculated average value was considered as the coating thickness. In order to ensure the uniformity of thickness, only the coating on the central area with a width about 40 mm was measured, while the other parts were scraped off. Considering that the size of coatings used in subsequent experiments were 100 mm in length and 20 mm in width, only the thickness variations in the width range of 20 mm of the measured results were selected to calculate the thickness at each position as shown as Fig. 1. The average thicknesses of coatings prepared by different molds were calculated and their densities also were estimated according to the coated amount and the size. The values of thickness and density were listed in Table 2. It can be found that these desiccant coatings prepared by the same mold have the comparable thicknesses.

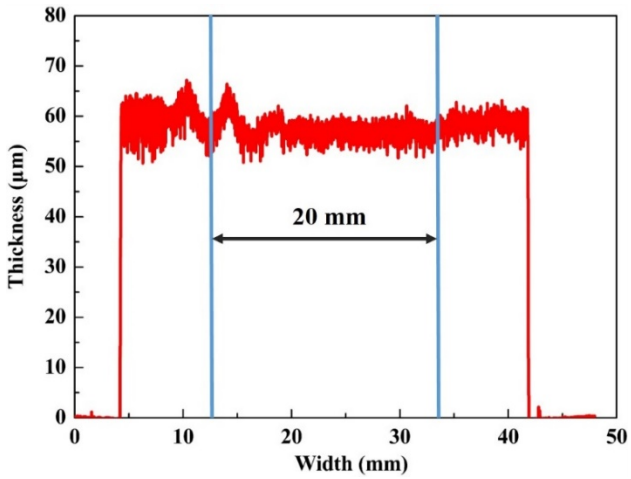

Fig. 1 Thickness variation at the width direction of silica gel coating prepared by the mold with bottom gap height of 0.1 mm

Table 2 Average thicknesses and densities of desiccant coatings prepared by different molds

Gap height of mold(mm)	Silica gel		FAM Z01		FAM Z05	
	Thickness (mm)	Density (kg/m^3)	Thickness (mm)	Density (kg/m^3)	Thickness (mm)	Density (kg/m^3)
0.1	0.0568	943.8	0.0399	872.2	0.0456	935.6
0.2	0.1325	708.2	0.1028	574.7	0.1147	628.0
0.3	0.1926	738.4	0.1694	698.0	0.1791	758.4
0.4	0.2502	775.3	0.2191	668.3	0.2704	528.2

2.3 Experimental apparatus and procedure

Experimental apparatus was designed to investigate the water uptake kinetics of desiccant coatings in approximate air channel of DCHEs. Schematic diagram of the experimental apparatus is shown in Fig. 2. The apparatus mainly consists of adsorber, adsorption/desorption temperature control unit, humidity control unit, flowmeter (Kofloc, Model 8550, Accuracy: ±1.5% F.S) and thermo-hygrometer (Vaisala, HUMICAP HMT-333, Accuracy: ±0.2 K, ±1%RH). The humidity control unit includes a low-temperature thermostat Th1 and two connected gas-washing bottles containing deionized water. The mixture gas of water vapor and N_2 produced after the dry N_2 flows through the gas-washing bottles is used to simulate the actual dehumidification air. The inlet air humidity of adsorber can reach target humidity by adjusting the temperature of thermostat Th1 according to the dew point temperature. The thermostat Th2 with a constant temperature of 30℃ is used to adjust the inlet air temperature and adsorption temperature of adsorber. Fig. 3 shows the structure diagram of adsorber made by aluminium. Two copper sheets coated with desiccant were pasted on the bottom surface of air channel of adsorber by using adhesive with high thermal conductivity.

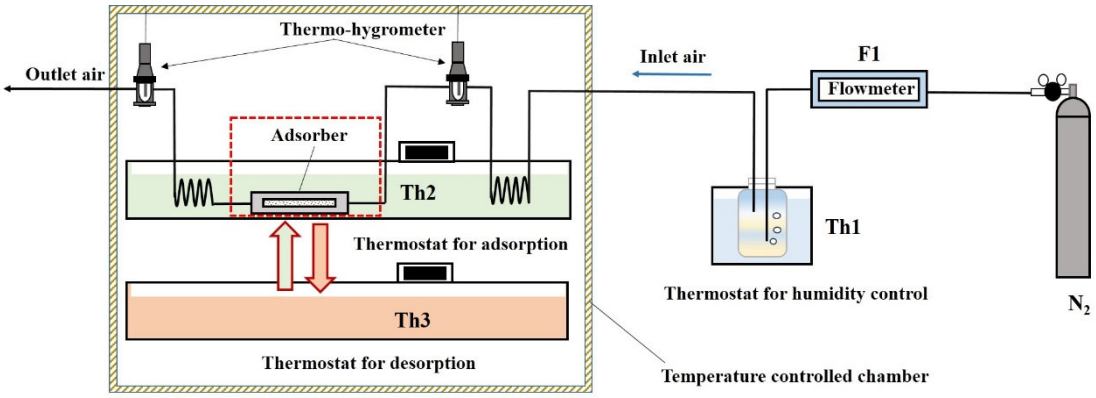

Fig.2 Schematic diagram of experimental apparatus

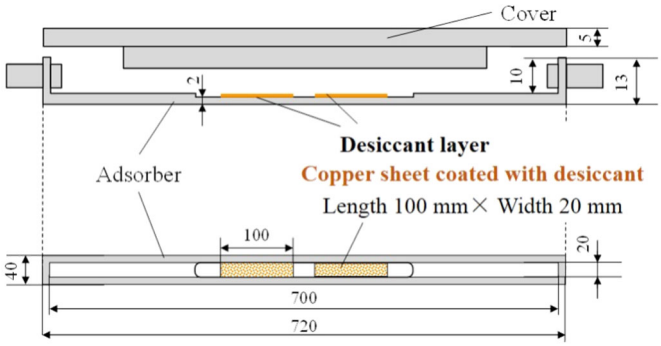

Fig.3 Structure diagram of adsorber

The main experiment procedures are as follow: Firstly, the desiccant coatings were dried in a vacuum drying oven at 100℃ for 8 hours before they were placed in the adsorber. The dry samples were weighed and the total weight of two pieces of coatings were recorded as m_1. Secondly, before the beginning of adsorption process, the volume flowrate $\dot{V}_a$ of N_2 was set as the required experiment value, and the inlet air humidity as well as temperature were adjusted to target values by using the thermostat Th1 and

Th2 respectively. After reaching steady state for the humidity and temperature, the adsorber was put into thermostat Th3 for desorption. Thirdly, when the desorption process reached equilibrium, the adsorber was removed from thermostat Th3 and put into thermostat Th2 for adsorption immediately. The transient variations of inlet and outlet air humidity were recorded by Agilent logger. Above adsorption and desorption processes were alternatively operated several times. Finally, the desiccant coatings were taken out and the desiccant layer on the surface of copper sheets were washed off. The net copper sheets were dried and weighed, and the total weight was recorded as m_2. The net weight of binder mixed desiccant was calculated as $m_1 - m_2$.

The inlet air velocity $u_{a,in}$ and water uptake change $|W - W_0|$ of coating were calculated by the following equations:

$$u_{a,in} = \frac{\dot{m}_a}{\rho_a A_{duct}} = \frac{\dot{V}_a}{A_{duct}} \tag{1}$$

$$|W - W_0| = \int_0^t |\Delta W|\, dt = \int_0^t \dot{m}_a \left| Y_{a,in} - Y_{a,out} \right| / (m_1 - m_2) dt \tag{2}$$

where A_{duct} is the inlet cross section of air channel of adsorber, ρ_a is the air density, $\dot{m}_a$ is the mass flowrate. $Y_{a,in}$ and $Y_{a,out}$ are the absolute humidity ratio at the inlet and outlet of adsorber. W_0 is the initial water uptake.

The error analysis of experimental results was evaluated by using the propagation of uncertainty [24]. The main independent variables, air relative humidity, temperature, flowrate and weight have measurement uncertainties of ±1%, ±0.2 K, ±1.5% F.S and ± 0.1mg respectively. These uncertainties finally translate into the uncertainty of Y_a and ΔW. In this study, the inlet and outlet air temperatures were regulated by thermostat Th2, so the temperatures both in the adsorption and desorption process can keep constant as the temperature of thermostat Th2. It should be noted that the uncertainty of Y_a calculated by relative humidity and temperature might rise significantly at low relative humidity due to dehumidification. Thus, the minimum outlet relative humidity was used to calculated the uncertainty of Y_a, it was less than ±3%. The change of uncertainty of ΔW was just attributed to the changes of air absolute humidity, flowrate and weight. Within the range of studied experimental parameters, the maximum uncertainty of ΔW was about ±13%.

3. Theoretical analysis

3.1 Kinetics evaluation

The linear driving force (LDF) model [25] was used to evaluate the water uptake kinetics. Its mathematical equations for adsorption and desorption process can be expressed as:

$$\frac{dW}{dt} = k_{ads}(W_{eq} - W) \tag{3}$$

$$\frac{dW}{dt} = k_{des}(W - W_0) \tag{4}$$

where $\frac{dW}{dt}$ means adsorption/desorption rate, k_{ads} and k_{des} are kinetic rate coefficient, W_0 and W_{eq} are the initial and equilibrium water uptake.

Integration of the above two equations and definition of dimensionless water

uptake $\theta = \frac{W-W_0}{W_{eq}-W_0}$, Eq. (5) and Eq. (6) were yielded:

$$\theta = \frac{W-W_0}{W_{eq}-W_0} = 1 - \exp(-k_{ads}t) \quad (5)$$

$$\theta = \frac{W-W_0}{W_{eq}-W_0} = \exp(-k_{des}t) \quad (6)$$

By using Eq. (5) and Eq. (6) to fit the experimental dimensionless water uptake curves, the key kinetic constants, i.e., adsorption/desorption rate coefficients k_{ads}/k_{des} can be determined. The kinetic constants are the overall description of mass transport characteristics. Studying their parameter dependence is vital to evaluate the mass transfer performance.

3.2 Adsorption isotherms

Water vapor adsorption isotherms of three desiccant coatings were evaluated by Belsorp 18 (Microtrac BEL, Japan) at 30℃ as shown in Fig. 4. It was observed that the equilibrium water uptake of silica gel coating gradually increased with the increase of relative humidity, and the isotherm showed a near-linear shape at low and medium relative humidity range. The Freundlich equation was selected to describe the isotherm of silica gel coating [11]:

$$W_{eq} = M\varphi^N \quad (7)$$

where the Freundlich constants M =0.265 and N =0.58 can be determined by fitting experimental equilibrium curve.

Compared to silica gel coating, FAM zeolites coatings have S-shaped isotherms. Fig. 4 shows that the equilibrium water uptakes were small at low relative humidity. However, with the increase of relative humidity, there was a steep gradient zone of equilibrium uptake change, which illustrated that the moisture concentration inside the coatings increased rapidly to equilibrium level. This phenomenon caused a much larger temperature effect on the equilibrium uptake when plotted as a function of relative humidity. The adsorption isotherms of FAM zeolites coatings can be described by the modified Langmuir equation in Ref. [26]:

$$W_{eq} = W_{max}\beta F/[1 + (\beta^{t_1} - \alpha)F^{t_1}]^{\frac{1}{t_1}} \quad (8)$$

where W_{max} is the maximum equilibrium uptake, $F = \varphi\exp\{\frac{m}{R_gT}(1-\varphi^n) + \mathrm{z}\}$. The physical interpretation of the coefficients β, m, n, t_1, α and z were illustrated in Ref. [26], they can be determined by fitting experimental equilibrium curves. In order to the convenience of numerical comparison, only one adsorption isotherm was used to determine the fitted parameters, although the adsorption isotherms of FAM zeolites were significant temperature dependent [27]. We just cared about whether the experimental adsorption isotherms can be covered by fitting curves, rather than the values and physical meaning of these fitted parameters. Table 3 listed the fitted parameters of Eq. (8) for isotherms of FAM Z01 and FAM Z05 coatings.

Table 3 Fitted parameters of isotherm equations for FAM zeolites coatings.

	W_{max}(kg/kg)	α	m (kJ/mol)	n	β	t_1	z	R^2
FAM Z01	0.19	0.002	120	-1	1	2	4.46	0.97

FAM Z05	0.21	0.01	100	-2	1	1.5	7.63	0.95

It was intelligible to find that all the experimental data can be well covered by the fitting curves in Fig. 4. The obtained isotherm equations provide reliable prediction of equilibrium water uptake, which facilitates to achieve the accurate numerical results in subsequent dehumidification simulation.

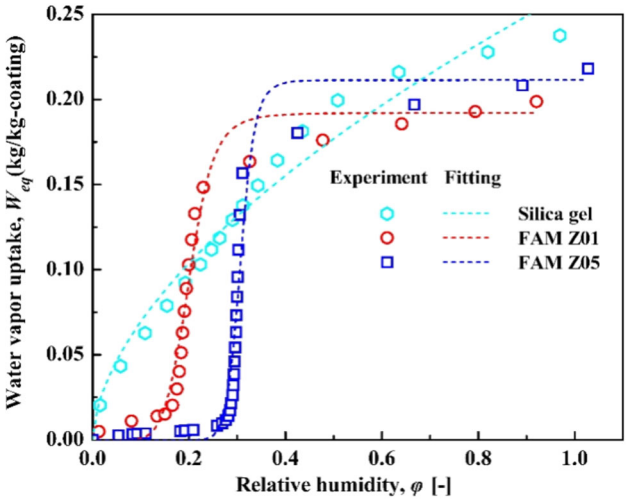

Fig. 4 Adsorption isotherms of three desiccant coatings at 30℃

4. Results and discussion

Dynamic water vapor adsorption/desorption characteristics of three desiccants coated adsorber were experimentally measured at various thickness and operating parameters listed as Table 2 and Table 4. One parameter was varied at one time to investigate its effect while all other parameters remained the same as the baseline values of Table 4. The thicknesses of samples prepared by the mold with bottom gap height of 0.2 mm was selected as baseline thickness. Other experimental operating parameters were listed in Table 4. All adsorption experiments were conducted under the same adsorption temperature 30℃.

Table 4 Various operating parameters

Parameters	Baseline values	Parametric variations
Inlet air velocity, m/s	1	1-3
Inlet air humidity, kg/kg	0.016 (60%RH)	0.012-0.020(45%-74%RH)
Regeneration temperature, ℃	60	50-80

Fig. 5 shows the typical results of outlet air humidity change in one cycle under baseline experiment conditions. It can be found that outlet humidity decreased rapidly to the lowest value at the initial stage of adsorption, and then increased gradually to inlet humidity. Conversely, the outlet humidity increased rapidly when desorption process was initiated. Afterwards, it decreased gradually until desorption equilibrium was achieved. Although the change curves were slightly different, all coatings can reach adsorption/desorption equilibrium in a relatively short time.

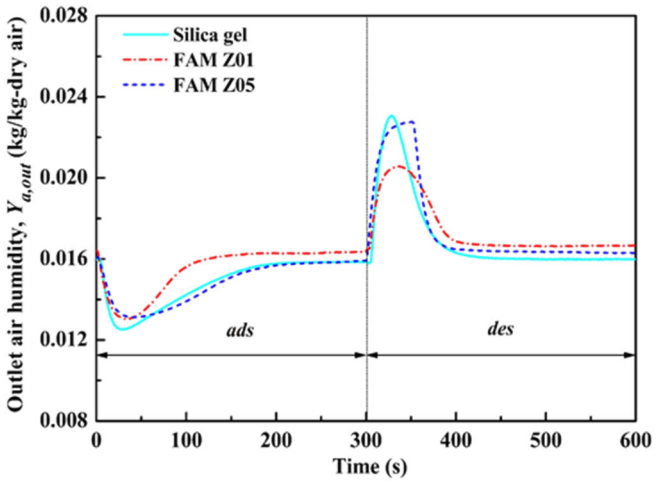

Fig. 5 Transient outlet air humidity of silica gel, FAM Z01 and FAM Z05 coated adsorber at baseline conditions

To further determine the optimized desiccant type under lower regeneration temperature, the dehumidification performance of silica gel, FAM Z01 and FAM Z05 coated air-cooled cross-flow DCHEs were numerically compared based on our previous validated mathematical model [28] under regeneration temperature range of 50-80°C. The two commonly employed performance indices, i.e., moisture removal capacity (MRC) and dehumidification performance of coefficient (DCOP) were investigated. The MRC represents that the difference of the time average humidity ratio between the inlet and outlet of DCHEs during adsorption process, while the DCOP reflects the ratio of latent heat dealing capacity to consumed regenerative heat. They were defined by the following equations:

$$MRC = \frac{1}{t}\int_0^t \left(Y_{a,ads,in} - Y_{a,ads,out}\right)dt \tag{9}$$

$$DCOP = \frac{\rho_{a,ads}\dot{V}_{a,ads}\Delta h_{vs}(Y_{a,ads,in}-Y_{a,ads,out})}{\rho_{a,des}\dot{V}_{a,des}(h_{a,des,in}-h_{a,ads,in})} = \frac{\rho_{a,ads}\dot{V}_{a,ads}\Delta h_{vs}(Y_{a,ads,in}-Y_{a,ads,out})}{\rho_{a,des}\dot{V}_{a,des}C_{pa}(T_{a,des,in}-T_{a,ads,in})} \tag{10}$$

4.1 Comparison of kinetics

4.1.1 Effect of inlet air humidity ratio

Fig. 6(a)-(c) describes the dynamic dimensionless water uptake curves of silica gel, FAM Z01 and FAM Z05 coated adsorber under various inlet air humidity of 0.012-0.020 kg/kg. It was observed that all desiccant coatings followed the similar adsorption kinetics pattern. The initial adsorption rate was higher, and then it declined gradually as the adsorption approached equilibrium. It also can be found that the curves of silica gel and FAM Z01 coatings were approximately overlapped at the first few seconds, while these of FAM Z05 coating were obviously lower. One explanation might simply be that the FAM Z05 coating had a larger effective adsorption capacity under the corresponding adsorption and regeneration conditions as listed in Table 5, where they were estimated by interpolation method according to the isotherms in Fig. 4. The LDF model fitting curves also were described in Fig. 6. It was observed that the fitting curves always were higher than the experiment results at the initial stage of adsorption process, but the opposite situation occurred at the final stage. The main reason for this deviation is that the initial stage of adsorber switching from desorption to adsorption was a non-

isothermal adsorption process, thus the LDF model developed by isothermal assumption resulted in an overestimation for the adsorption capacity. Nevertheless, the current experiments can be considered as a near-isothermal adsorption process where the initial non-isothermal stage was relative short under a good cooling effect. The experiment results still could be well covered by fitting curves, and the correlation coefficient R^2 of all fitting curves were greater than 0.95.

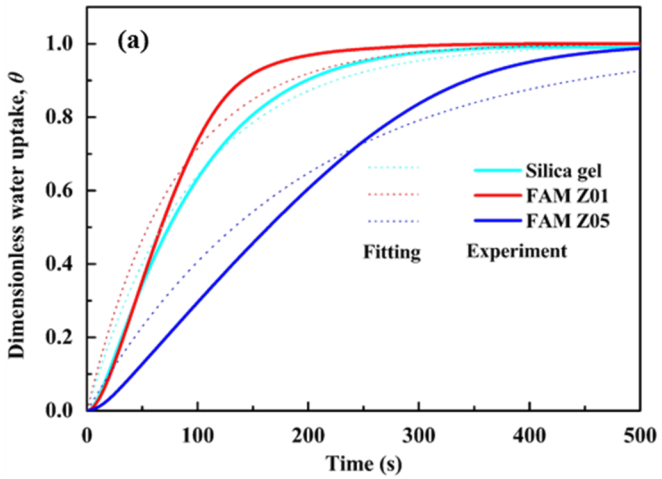

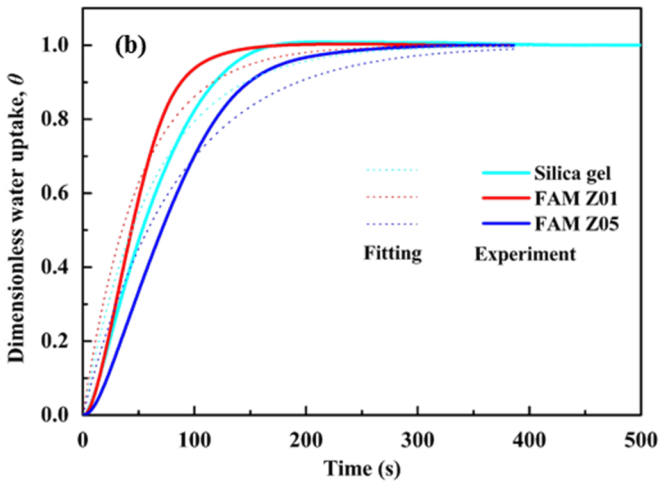

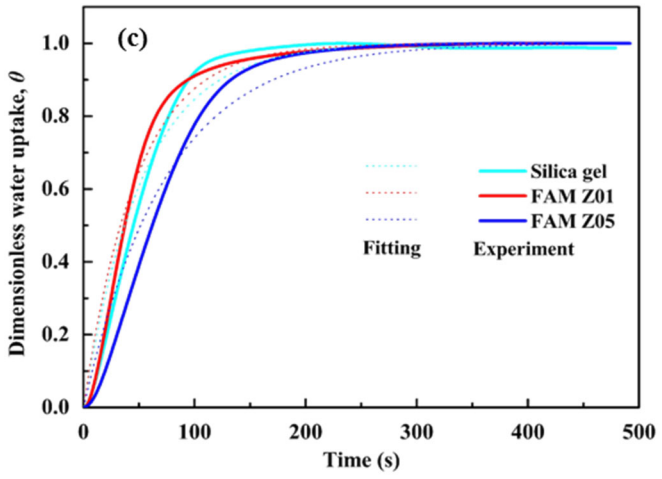

Fig. 6 Dynamic dimensionless water uptake curves of silica gel, FAM Z01 and FAM Z05 coated adsorber under various inlet air humidity: (a) 0.012 kg/kg; (b) 0.016 kg/kg; (c) 0.020 kg/kg.

Table 5 Theoretical effective adsorption capacity of desiccant coating

Inlet air humidity (kg/kg)	Adsorption capacity (kg/kg)		
	Silica gel	FAM Z01	FAM Z05
0.012	0.1294	0.1623	0.1785
0.016	0.1448	0.1701	0.1883
0.020	0.1455	0.1751	0.1960

It can be seen from Fig. 7 that the adsorption rate coefficients k_{ads} of silica gel, FAM Z01 and FAM Z05 coatings increased with the increase of inlet air humidity. This is easily understood because the higher air humidity was, the higher the water vapor pressure over the desiccant coatings was, the larger adsorption driving force had. An intuitive comparison from Fig. 7 shows that the average k_{ads} of FAM Z01 coating was the largest, followed by silica gel coating, and that of FAM Z05 coating was the smallest. However, one noticeable point was that, even though the k_{ads} was considered as a criterion for the adsorption rate, the effective adsorption capacity as listed in Table 5 also can be a dominant factor restricting adsorption rate [29]. Therefore, it was difficult to justify that the adsorption rate of FAM Z01 coating was superior to the other two coatings in terms of k_{ads}. Nevertheless, these fitted k_{ads} were more representative than those results obtained by static adsorption experiments, and they truly reflected the overall mass transfer performance in the open dehumidification air channel.

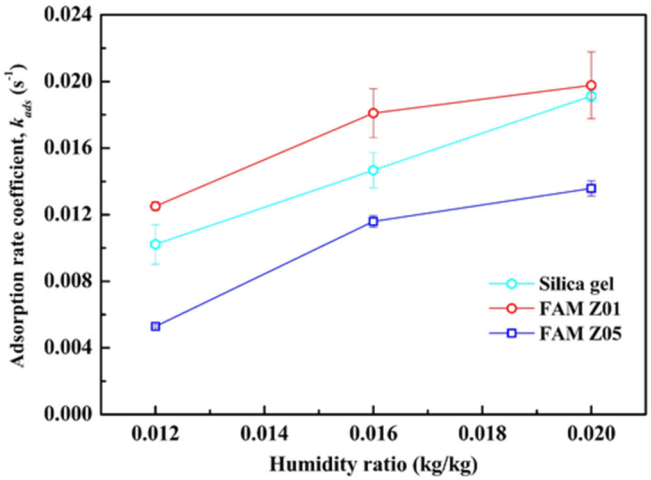

Fig. 7 Adsorption rate coefficients k_{ads} of silica gel, FAM Z01 and FAM Z05 coatings under various inlet air humidity

4.1.2 Effect of inlet air velocity

Fig. 8(a)-(c) describes the dynamic dimensionless water uptake curves of silica gel, FAM Z01 and FAM Z05 coated adsorber under various inlet air velocity of 1-3m/s. The overall mass transfer behavior of desiccant coated adsorber was controlled by the

air- and solid-side mass transfer resistances. According to Ref. [30], the overall mass transfer coefficient is the function of Reynolds, temperature and absorbed water uptake. Due to near-isothermal adsorption, it seemed that the increasing Reynolds dominated the enhancement of overall mass transfer. As it can be found that the higher air velocity, the steeper dynamic water uptake curves and the faster rate to reach adsorption equilibrium. All fitted curves still were higher than the experiment results at the initial stage of adsorption process but lower at the final stage. The time corresponding to the intersection points of fitting curves and experiment results became smaller with the increase of air velocity, which illustrated the effect of residual heat when adsorber switching from desorption to adsorption was eliminated faster under higher air velocity. The minimum correlation coefficients R^2 of all fitting curves of LDF model was 0.94.

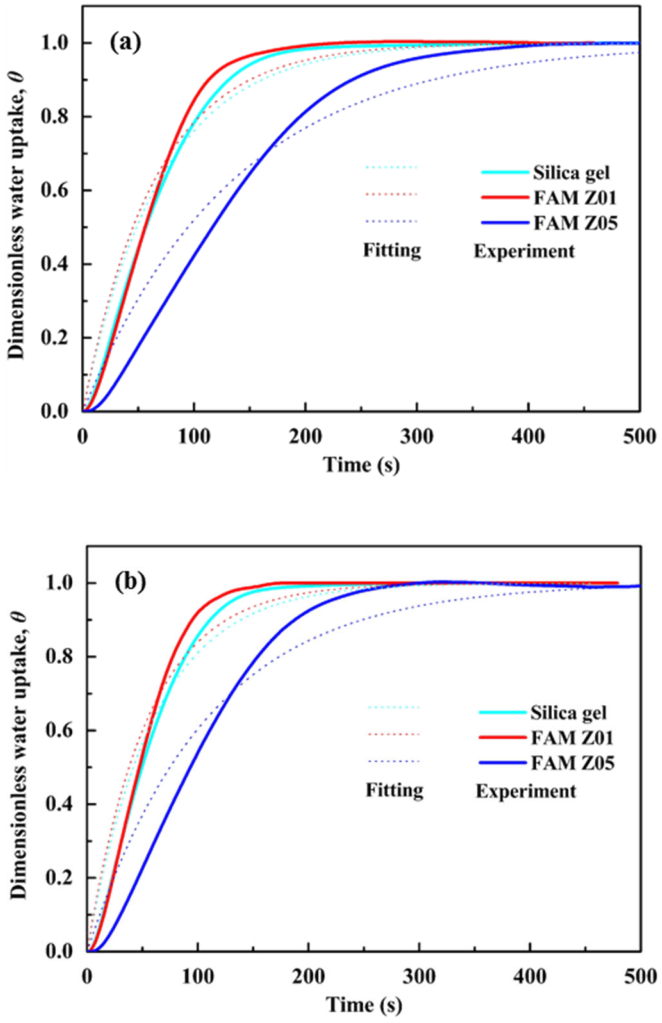

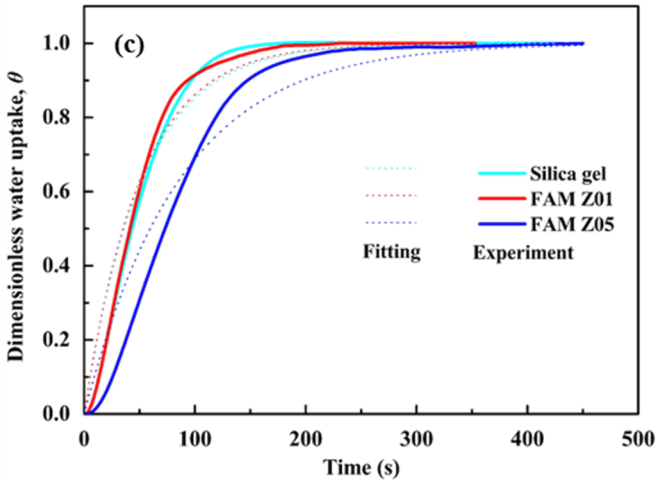

Fig. 8 Dynamic dimensionless water uptake curves of silica gel, FAM Z01 and FAM Z05 coated adsorber under various inlet air velocity: (a) 1 m/s; (b) 2 m/s; (c) 3 m/s.

Fig. 9 shows the almost linear changes of adsorption rate coefficients k_{ads} with increasing air velocity. This fact also supported the above conclusion that the enhancement of overall mass transfer was dominated by the increasing Reynolds. The silica gel and FAM Z01 coatings possessed a comparable k_{ads} at the corresponding air velocity, their average k_{ads} increased from 0.0147 s^{-1} to 0.019 s^{-1} and 0.0148 s^{-1} to 0.0205 s^{-1} respectively when the air velocity increased from 1m/s to 3 m/s. By comparison, an obviously smaller k_{ads} for FAM Z05 coating was observed, which increased from 0.0076 s^{-1} to 0.0127 s^{-1}. These obvious effects of air velocity on k_{ads} demonstrated that the air-side mass transfer resistance still played an important role in the overall mass transfer process under current coating thickness.

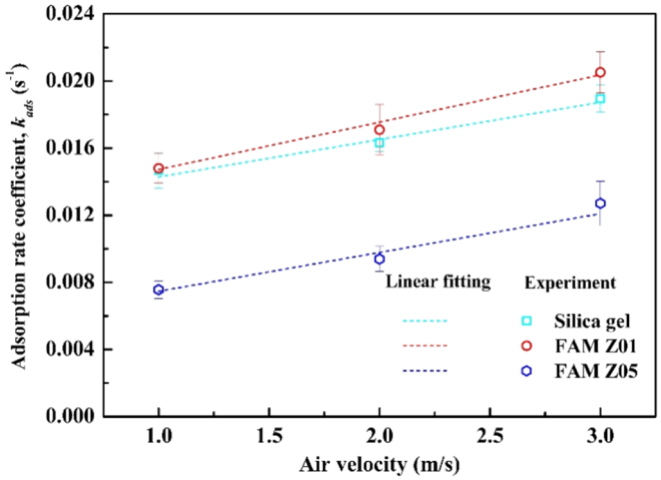

Fig. 9 Adsorption rate coefficients k_{ads} of silica gel, FAM Z01 and FAM Z05 coatings under various inlet air velocity.

4.1.3 Effect of regeneration temperature

Dynamic water adsorption/desorption uptake curves of silica gel, FAM Z01 and FAM Z05 coated adsorber under various regeneration temperature were depicted in Fig. 10. Due to the fact that the adsorber obtained a good cooling after switching from

desorption to adsorption, the regenerative residual heat can be eliminated in time. Three desiccant coatings showed similar adsorption kinetics even for various regeneration temperatures. A rapid decrease of water uptake was observed for the three desiccants coated adsorber at the initial stage of desorption process and then it slowly declined, but the decrease was relative gentle at regeneration temperature of 50°C. The good agreement between experiment results and fitting curves also was observed in Fig. 10, and the minimum correlation coefficients R^2 of fitting curves of adsorption and desorption were 0.94 and 0.93 respectively.

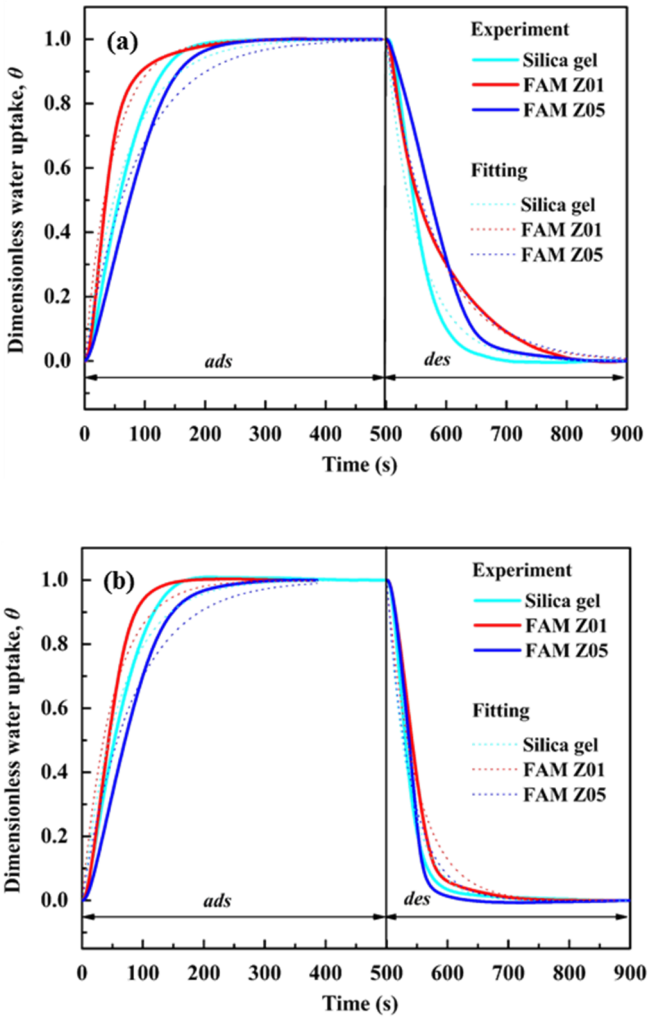

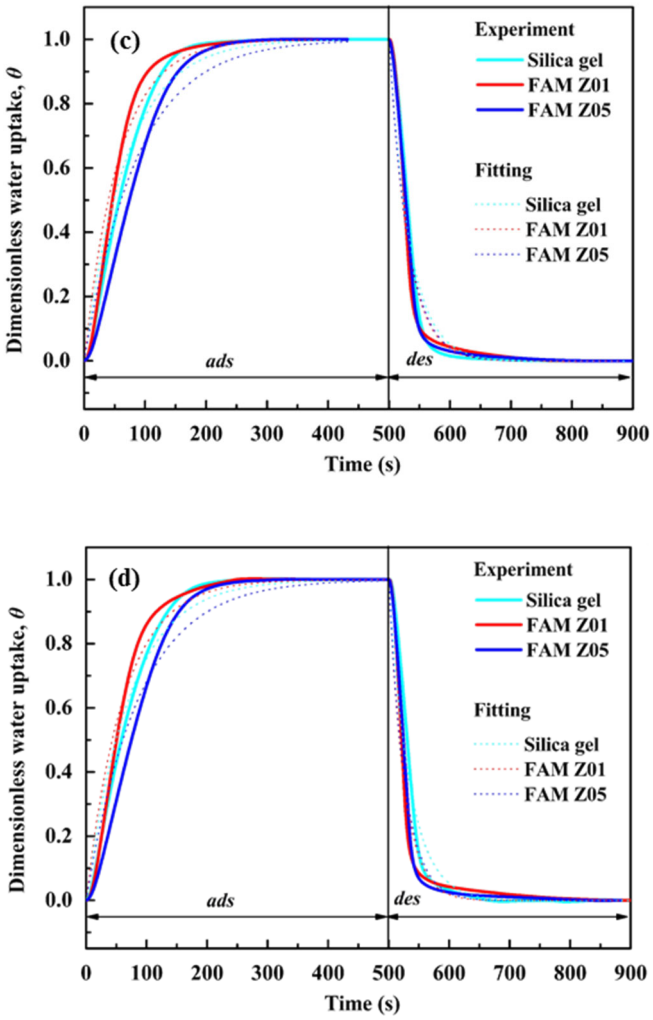

Fig. 10 Dynamic dimensionless water adsorption/desorption curves of silica gel, FAM Z01 and FAM Z05 coated adsorber under various regeneration temperature: (a) 50℃; (b) 60℃; (c) 70℃; (d) 80℃.

Table 6 Theoretical effective adsorption capacity of desiccant coating

Regeneration temperature	Adsorption capacity (kg/kg)		
(℃)	Silica gel	FAM Z01	FAM Z05
50	0.1166	0.0790	0.1867
60	0.1448	0.1701	0.1883
70	0.1598	0.1723	0.1891
80	0.1727	0.1750	0.1898

The adsorption/desorption rate coefficients k_{ads}/k_{des} of three desiccant coatings under various regeneration temperature were depicted in Fig. 11. In current study, the corresponding air relative humidity decreased from 0.2 to 0.05 when regeneration temperature increased from 50℃ to 80℃. According to Table 6, the FAM zeolites coatings can be regenerated well under all regeneration temperature except FAM Z01 coating at regeneration temperature of 50℃. It seemed that the effective adsorption capacity of FAM zeolites coatings dominated the adsorption kinetics because their

k_{ads} maintained a slight change as that of effective adsorption capacity. Notably, the k_{ads} of silica gel coating did not show obvious dependence on the increasing effective adsorption capacity and it almost maintained a constant value. These different adsorption characteristics could be attributed to the effect of adsorption isotherm shape. Likewise, different desorption behaviors also were observed in Fig. 11. When the regeneration temperature was in the range of 50-60℃, the highest average k_{des} was found for silica gel coating and these of FAM Z01 coating were the smallest, while the results were exactly contrary in the regeneration temperature range of 70-80℃.

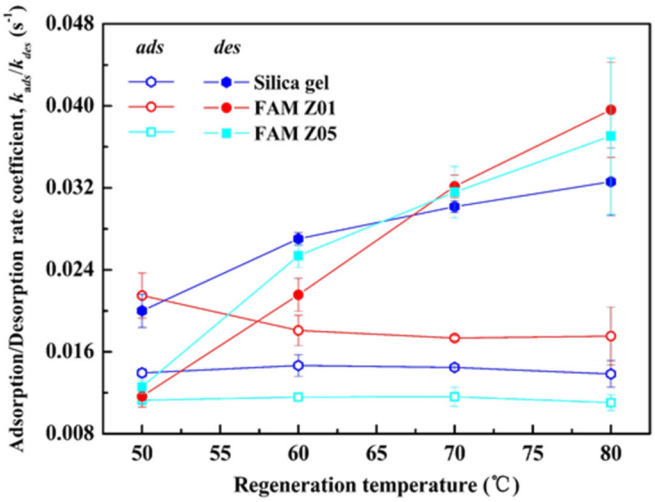

Fig. 11 Adsorption/desorption rate coefficients k_{ads}/k_{des} of silica gel, FAM Z01 and FAM Z05 coatings under various regeneration temperature

4.1.4 Effect of coating thickness

The dynamic water uptake curves of silica gel, FAM Z01 and FAM Z05 coated adsorber with various coating thickness were described as Fig. 12. In general, the diffusion resistance and non-isothermal effect were the two limiting mechanisms of adsorption kinetics [31]. In current study, the diffusion resistance should be considered as the main factor restricting the adsorption kinetics due to good cooling effect. The thicker the desiccant coating, the greater the moisture transfer resistance and the slower adsorption kinetics as shown in Fig. 12. The LDF model based on isothermal adsorption assumption was still applicable for capturing the experiment results. The minimum correlation coefficients R^2 of fitting curves was 0.95.

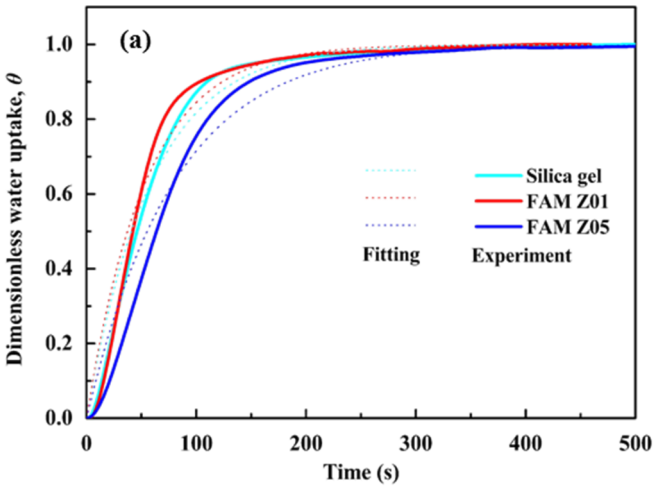
(a)
Dimensionless water uptake, θ
Time (s)
Silica gel
FAM Z01
FAM Z05
Fitting
Experiment

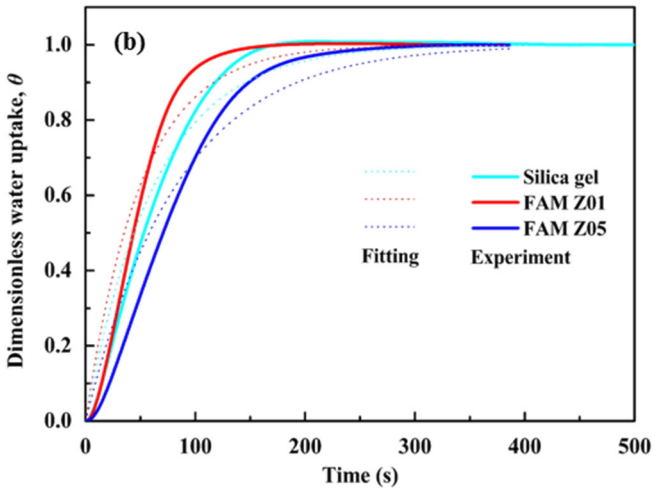
(b)
Dimensionless water uptake, θ
Time (s)
Silica gel
FAM Z01
FAM Z05
Fitting
Experiment

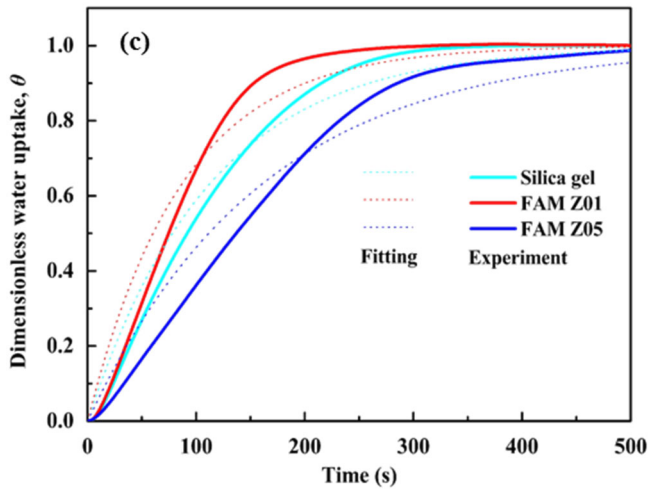
(c)
Dimensionless water uptake, θ
Time (s)
Silica gel
FAM Z01
FAM Z05
Fitting
Experiment

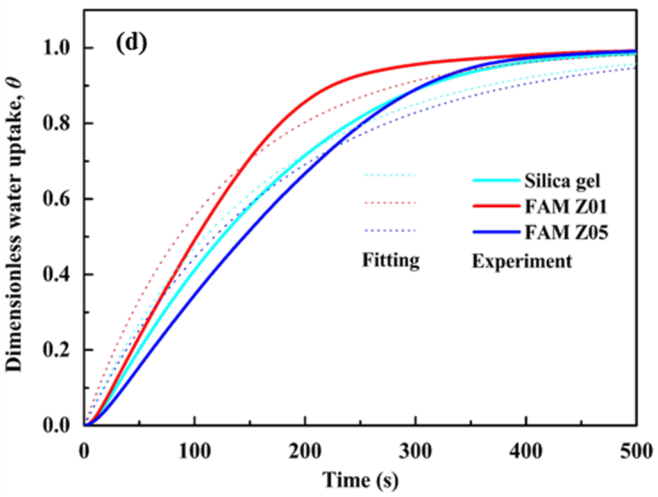

Fig. 12 Dynamic dimensionless water uptake curves of silica gel, FAM Z01 and FAM Z05 coatings prepared by different molds with various bottom gap height: (a) 0.1 mm; (b) 0.2 mm; (c) 0.3 mm; (d) 0.4 mm.

Fig. 13(a) describes the change of adsorption rate coefficients k_{ads} of three desiccant coatings under various thicknesses. There were two effects caused by the increasing thickness: one was larger water adsorption amount due to more desiccant, and the other was larger heat and mass transfer resistance. Both of them could increase the adsorption equilibrium time and decrease the k_{ads}. It can be seen that these k_{ads} declined with different extents as the thickness increased. According to the reference [32], the average internal effective diffusion coefficient (D_e) of plane desiccant layer in adsorption process can be calculated by $D_e = \frac{\bar{k}_{ads}\delta^2}{3}$. The changes of D_e in silica gel, FAM Z01 and FAM Z05 coatings were illustrated in Fig. 13(b). It was observed that the D_e rose almost linearly with the increase of thickness for all desiccant coatings. Thus, the D_e can be fitted by the linear equation of $D_e = C\delta$, where the value of $C = \frac{\bar{k}_{ads}\delta}{3}$ was a constant. The fitted values of C for silica gel, FAM Z01 and FAM Z05 coatings were 5.54×10^{-10}, 5.90×10^{-10} and 4.43×10^{-10}, respectively. These results provided a simple way to predict the value of $\bar{k}_{ads}$ when the coating thickness was determined.

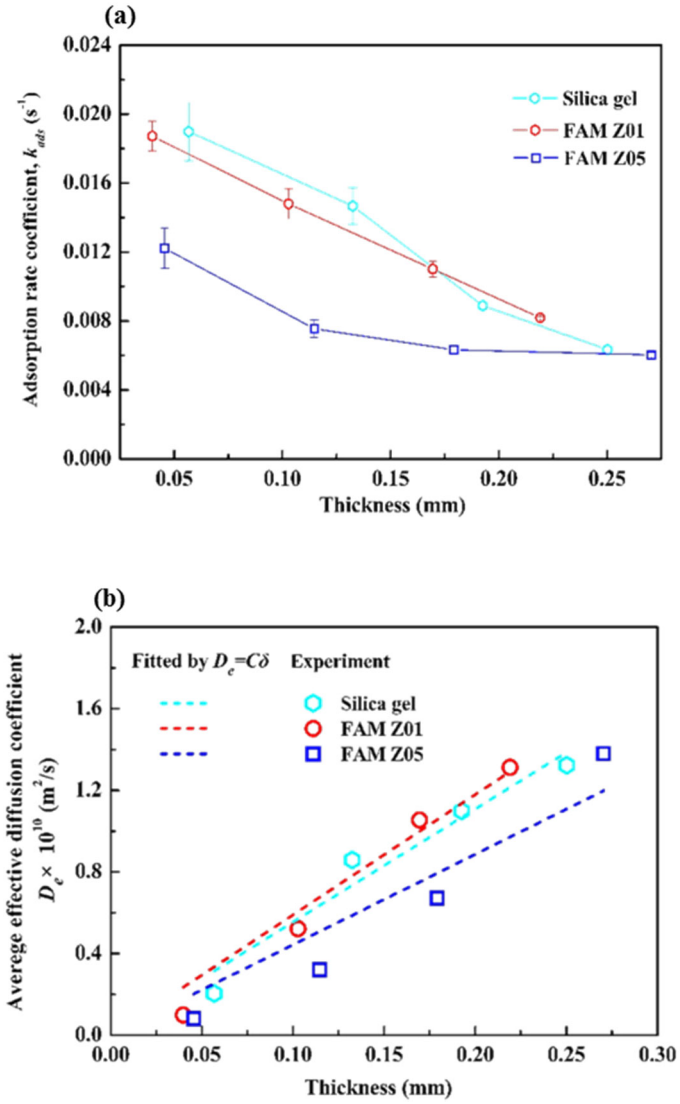

Fig. 13 Adsorption rate coefficients k_{ads} and average effective mass transfer coefficients D_e of silica gel, FAM Z01 and FAM Z05 coatings under various coating thickness: (a) k_{ads}; (b) D_e.

4.2 Comparison of dehumidification performance

In this section, the dehumidification performances of silica gel, FAM Z01 and FAM Z05 coated air-cooled cross-flow DCHEs were numerically investigated under the low regeneration temperature range of 50-80℃. The cooling air velocity and temperature in DCHEs were selected as 4 m/s and 30℃ to achieve a good isothermal cooling effect. The length of desiccant coated dehumidification channel was 0.2 m same to the current experiment. The air velocities for adsorption and regeneration were fixed at 1 m/s. All of the inlet air humidity ratio were selected as 0.016 kg/kg. The average densities of coatings were estimated by the results in Table 2. The values of specific heat and thermal conductivity of FAM Z01 and FAM Z05 were set to be equal because they had similar structure. The adsorption heat of FAM Z01 and FAM Z05 were assumed to be 3030 kJ/kg and 2800 kJ/kg according to the Ref. [33]. Table 7 listed the key simulated input parameters. In order to ensure the same amount of desiccant in DCHEs, the thickness of FAM Z01 coating was first selected as 0.1 mm,

and then the thicknesses of silica gel and FAM Z05 coatings were estimated as 0.088 mm and 0.099 mm respectively according to the coating density and geometric structure of air channel in DCHEs [28]. Such a low thickness can ignore the mass transfer resistance in desiccant layer for numerical modelling [34]. The effective mass fractions of all coatings were assumed as 0.9. Different cycle times (300 s and 600 s) were simulated. A fully long regeneration process under the corresponding regeneration conditions was firstly simulated and the final states were set as the initial states of the first dehumidification cycle. Three dehumidification cycles were calculated and the numerical results of the third cycle were used to calculate the dehumidification performance, i.e., MRC and DCOP.

Table 7 Input parameters of different coatings

Properties	Silica gel	FAM Z01	FAM Z05
Density	791.5 kg/m^3	703.3 kg/m^3	712.6 kg/m^3
Specific heat	921 J/kg·K	805 J/kg·K	805 J/kg·K
Thermal conductivity	0.198 W/m·K	0.113 W/m·K	0.113 W/m·K
Adsorption heat	2650 kJ/kg	3030 kJ/kg	2800 kJ/kg
Pore diameter	2.4 nm	0.73 nm	0.73 nm

The comprehensive effect of desiccant properties (kinetics and isotherm) on dehumidification performance can be analyzed based on the comparable standard due to the same desiccant amount and negligible intralayer mass transfer resistance through numerical simulation. Fig. 14 shows the transient change of outlet air humidity of silica gel, FAM Z01 and FAM Z05 coated DCHEs under regeneration temperature of 50°C and 80°C for various cycle times. Compared to the first dehumidification cycle, all minimum values of outlet air humidity increased as the cycle progresses. It was illustrated that these desiccant coatings were not able to achieve full regeneration under the investigated regeneration conditions. For a fixed cycle time, if the desorption rate is less than the adsorption rate, the dehumidification capacity of the DCHEs might gradually decay with the progress of the cycle such as the FAM Z01 and FAM Z05 coated DCHEs in Fig. 14(a) and Fig. 14(c), but these decays would eventually reach equilibrium and stable cycle could be achieved. With the increase of regeneration temperature, the desorption rate increased and the better regeneration was achieved, there was a relatively stable cycle for the transient change of outlet air humidity after the first cycle as shown in Fig. 14(b) and Fig. 14(d). It is worth noting that the transient change of outlet humidity of silica gel coated DCHE always could maintain a stable periodicity under different regeneration temperatures and cycle times, this can be attributed to the near linear-shape adsorption isotherm of silica gel coating. By comparing the Fig. 14(a)-(d), it can be inferred that the appropriate cycle time and regeneration temperature should be ensured for the stable and efficient operation of DCHEs, and they might be various for different desiccant types DCHEs.

(a)

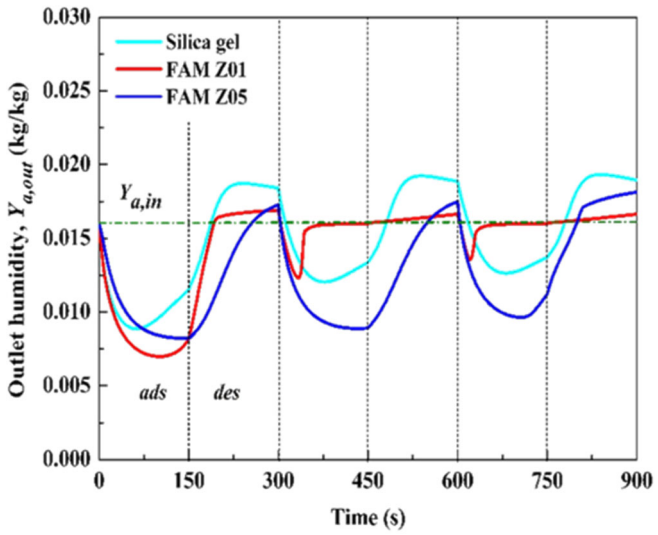
Silica gel
FAM Z01
FAM Z05
$Y_{a,in}$
ads
des
Outlet humidity, $Y_{a,out}$ (kg/kg)
Time (s)
0.030
0.025
0.020
0.015
0.010
0.005
0.000
0
150
300
450
600
750
900

(b)

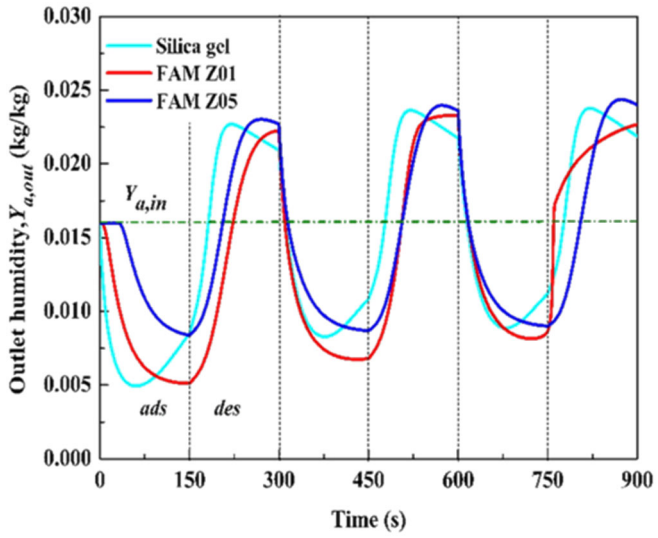
Silica gel
FAM Z01
FAM Z05
$Y_{a,in}$
ads
des
Outlet humidity, $Y_{a,out}$ (kg/kg)
Time (s)
0.030
0.025
0.020
0.015
0.010
0.005
0.000
0
150
300
450
600
750
900

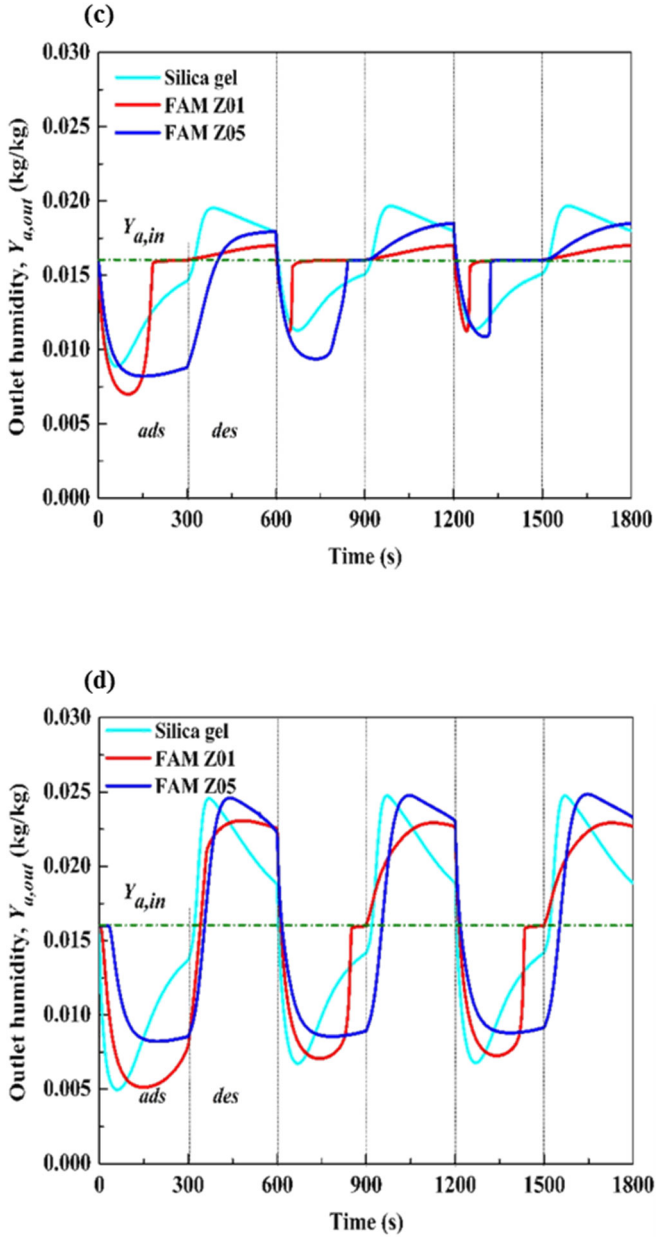

Fig. 14 Transient change of outlet air humidity of silica gel, FAM Z01 and FAM Z05 coated DCHEs: (a) regeneration temperature 50℃ and cycle time 300 s; (b) regeneration temperature 80℃ and cycle time 300 s; (c) regeneration temperature 50℃ and cycle time 600 s; (d) regeneration temperature 80℃ and cycle time 600 s.

Effect of regeneration temperature on MRC and DCOP of silica gel, FAM Z01 and FAM Z05 coated DCHEs under various cycle times was presented in Fig. 15. Generally, the higher regeneration temperature, the better desorption of DCHEs and the higher MRC as shown in Fig. 15(a) and Fig. 15(c). However, there was an exception for FAM Z05 coated DCHE under cycle time of 300 s. It can be explained that the residual heat of regeneration process was difficult to be released in relatively short cycle time when the cycle was switched, which seriously affected the moisture removal of FAM Z05 coating during adsorption process due to its low adsorption capacity in wider range. With the increase of regeneration temperature, the MRC of FAM Z01 coated DCHE

increased to even be higher than these of the other two DCHEs under regeneration temperature of 80℃ and cycle time of 300 s. The different change trends of DCOP for three desiccant types DCHEs also were observed from Fig. 15(b) and Fig. 15(d). The silica gel coated DCHE had a decreased DCOP with the increasing regeneration temperature for various cycle times, while a totally opposite change trend of DCOP for FAM Z01 coated DCHE was observed. It should be noted that the DCOP of FAM Z05 coated DCHE could achieve a peak value at the regeneration temperature of 70℃ and cycle time of 600 s, while it gradually decreased with the increasing regeneration temperature for the cycle time of 300 s. In summary, the difference of dehumidification performance of the three desiccant types DCHEs became smaller as regeneration temperature increased. FAM Z05 coated DCHE achieved better dehumidification performance at low regeneration temperature and short cycle time, its MRC and DCOP could reach 0.495 g/kg and 0.57 at the regeneration temperature of 50℃ and cycle time of 300 s, which were 2.3 and 15.4 times higher than these of silica gel and FAM Z01 coated DCHEs, respectively. Different from Ref. [16], the dehumidification performance of silica gel coated DCHE in current study was even better than FAM Z05 coated DCHE at the regeneration temperature of 50℃ and cycle time of 600 s, but its DCOP was only 0.29 which was significantly lower than the corresponding DCOP of FAM Z05 coated DCHE at cycle time of 300 s. Therefore, from the perspective of efficient utilization of lower temperature heat energy, FAM Z05 was more promising than FAM Z01 and silica gel in air-cooled DCHE systems especially at low regeneration temperature less than 50℃.

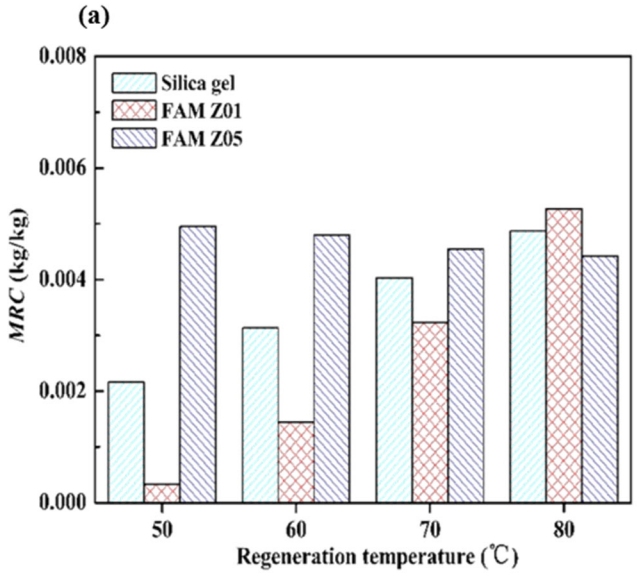

(b)

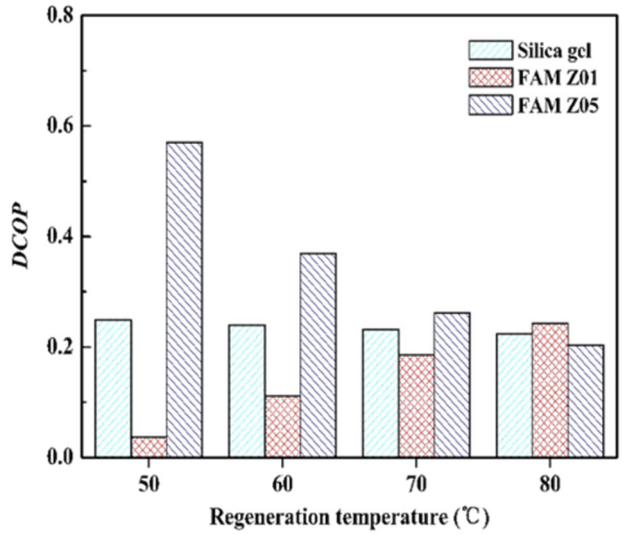
0.8
0.6
0.4
0.2
0.0
DCOP
Silica gel
FAM Z01
FAM Z05
50
60
70
80
Regeneration temperature (℃)

(c)

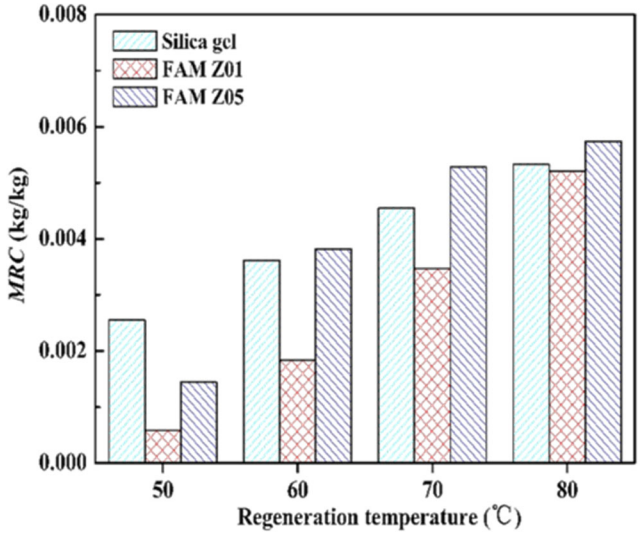
0.008
0.006
0.004
0.002
0.000
MRC (kg/kg)
Silica gel
FAM Z01
FAM Z05
50
60
70
80
Regeneration temperature (℃)

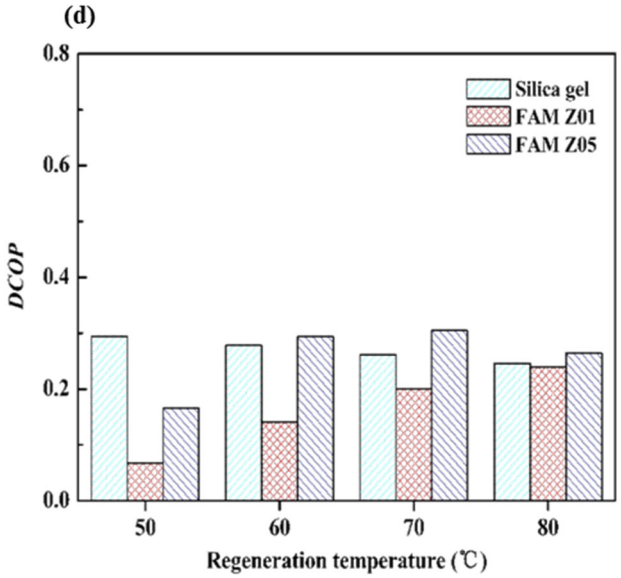

Fig. 15 Effect of regeneration temperature on MRC and DCOP of silica gel, FAM Z01 and FAM Z05 DCHEs under various cycle times: (a) MRC under cycle time 300 s; (b) DCOP under cycle time 300 s; (c) MRC under cycle time 600 s; (d) DCOP under cycle time 600 s.

5. Conclusion

In this study, the water uptake kinetics of silica gel and two aluminophosphate zeolites (FAM Z01 and FAM Z05) coated adsorber were investigated under various parameter conditions. The dehumidification performances of three desiccant types air-cooled DCHEs also were simulated at the low regeneration temperature range of 50-80°C. The conclusions mainly included:

(1) The experimental dynamic dimensionless water uptake results of silica gel, FAM Z01 and FAM Z05 coated adsorber could be well covered by the fitting curves of LDF model. The fitting curves were higher than the experiment results at the initial stage of adsorption process, but the opposite situation occurred at the final stage.

(2) The inlet air humidity ratio, regeneration temperature, air velocity and coating thickness affected the adsorption rate coefficient k_{ads}. The k_{ads} increased with the increase of air humidity and air velocity, but decreased with increasing coating thickness. It is worth pointing out that the increasing regeneration temperature had a little effect on the k_{ads}, while the desorption rate coefficient k_{des} increased significantly.

(3) The moisture removal capacity (MRC) and dehumidification performance of coefficient (DCOP) of the three desiccant types DCHEs showed different change trends as regeneration temperature increased under various cycle times (300s and 600s). Almost all MRCs were gradually increased except that of FAM Z05 coated DCHE at the short cycle time. Silica gel coated DCHE had a decreased DCOP, while that of FAM Z01 coated DCHE was increased. It should be noted that the DCOP of FAM Z05 coated DCHE could achieve a peak value at regeneration temperature of 70°C and cycle time of 600 s, while the DCOP gradually decreased under the short cycle time. Simulated results also showed that the MRC and DCOP of FAM Z05 coated DCHE could reach

0.495 g/kg and 0.57 at the regeneration temperature of 50℃ and cycle time of 300 s, which were 2.3 and 15.4 times higher than these of silica gel and FAM Z01 coated DCHEs, respectively. It demonstrated that the FAM Z05 was more promising to utilize the lower-grade heat energy with temperature less than 50℃.

Conflict of Interest

None declared.

Acknowledgements

This work was supported by Key-Area Research and Development Program of Guangdong Province (2020B0202010004). This research also was partially supported by Fuji Science and Technology Foundation, Key Special Project for Introduced Talents Team of Southern Marine Science and Engineering Guangdong Laboratory (Guangzhou) (GML2019ZD0108) and Science and Technology Program of Guangzhou, China (202102020235).

References

[1] A. Abela, L. Hamilton, R. Hitchin, et al. Study on Energy Use by Air-Conditioning: Final Report[R]. BRE Client Report-for the Department of Energy and Climate Change, HPR218-1001 June 2016.

[2] M. A. Mandegari, S. Farzad, G. Angrisani, et al. Study of purge angle effects on the desiccant wheel performance[J]. Energy Conversion and Management, 2017, 137: 12-20.

[3] N. Asim, M. H. Amin, M. A. Alghoul, et al. Key Factors of Desiccant-Based Cooling Systems: Materials[J]. Applied Thermal Engineering, 2019, 159: 113946.

[4] F. Ge, C. Wang. Exergy analysis of dehumidification systems: A comparison between the condensing dehumidification and the desiccant wheel dehumidification[J]. Energy Conversion and Management, 2020, 224: 113343.

[5] X. G. Xu, Z. W. Zhong, S. M. Deng, et al.. A review on temperature and humidity control methods focusing on air-conditioning equipment and control algorithms applied in small-to-medium-sized buildings[J]. Energy and Buildings, 2018, 162: 163-176.

[6] P. Vivekh, M. Kumja, D. T. Bui, et al. Recent developments in solid desiccant coated heat exchangers – A review[J]. Applied Energy, 2018, 229: 778-803.

[7] X. Zheng, T. S. Ge, R. Z. Wang. Recent progress on desiccant materials for solid desiccant cooling systems[J]. Energy, 2014, 74: 280-294.

[8] P. Vivekh, D. T. Bu I, M. R. Islam, et al. Experimental performance evaluation of desiccant coated heat exchangers from a combined first and second law of thermodynamics perspective[J]. Energy Conversion and Management, 2020, 207: 112518.

[9] M. Sultan, T. Miyazaki, S. Koyama. Optimization of adsorption isotherm types for desiccant air-conditioning applications[J]. Renewable Energy, 2018, 121: 441-450.

[10] S. H. Seol, K. Nagano, J. Togawa. A new experimental method to separate

interfacial and internal mass transfer on coated adsorbent[J]. Applied Thermal Engineering, 2019, 159: 113869.
[11] S. W. Hong, S. H. Ahn, J. D. Chung, et al. Characteristics of FAM-Z01 compared to silica gels in the performance of an adsorption bed[J]. Applied Thermal Engineering, 2016, 104: 24-33.
[12] M. Intini, M. Goldsworthy, S. White, et al. Experimental analysis and numerical modelling of an AQSOA zeolite desiccant wheel[J]. Applied Thermal Engineering, 2015, 80: 20-30.
[13] A. Akisawa, M. Umair, K. Enoki, et al. Static analysis of a new scheme of two stage refrigeration cycle with the combination of FAM Z01 and FAM Z05 adsorbents[J]. International Journal of Refrigeration, 2018, 92: 143-153.
[14] S. Kayal, B. Sun, B. B. Saha. Adsorption characteristics of AQSOA zeolites and water for adsorption chillers[J]. International Journal of Heat and Mass Transfer, 2016, 92: 1120-1127.
[15] S. Shimooka, K. Oshima, H. Hidaka, et al. The Evaluation of Direct Cooling and Heating Desiccant Device Coated with FAM[J]. Journal of Chemical Engineering of Japan, 2007, 40(13): 1330-1134.
[16] X. Zheng, R. Z. Wang, T. S. Ge, et al. Performance study of SAPO-34 and FAPO-34 desiccants for desiccant coated heat exchanger systems[J]. Energy, 2015, 93(1): 88-94.
[17] M. Kubota, N. Hanaoka, H. Matsuda, et al. Dehumidification behavior of cross-flow heat exchanger type adsorber coated with aluminophosphate zeolite for desiccant humidity control system[J]. Applied Thermal Engineering, 2017, 122: 618-625.
[18] B. Sun, A. Chakraborty. Thermodynamic frameworks of adsorption kinetics modeling: Dynamic water uptakes on silica gel for adsorption cooling applications[J]. Energy, 2015, 84: 296-302.
[19] Y. D. Tu, R. Z. Wang, T. S. Ge. Moisture uptake dynamics on desiccant-coated, water-sorbing heat exchanger[J]. International Journal of Thermal Sciences, 2018, 126: 13-22.
[20] Y. D. Tu, R. Z. Wang, T. S. Ge, et al. Comfortable, high-efficiency heat pump with desiccant-coated, water-sorbing heat exchangers[J]. Scientific Reports, 2017, 7: 40437.
[21] Y. D. Tu, R. Z. Wang, L. J. Hua, et al. Desiccant-coated water-sorbing heat exchanger: Weakly-coupled heat and mass transfer[J]. International Journal of Heat and Mass Transfer, 2017, 113: 22-31.
[22] E. Glueckauf. Theory of chromatography. Part 10.—Formul for diffusion into spheres and their application to chromatography[J]. Transactions of the Faraday Society, 1955, 51: 1540-1551.
[23] M. Kubota, S. Shibata, H. Matsuda. Water adsorption characteristics of desiccant humidity controlling system with cross-flow type heat exchanger adsorber (In Japanese)[J]. Trans. Jpn Soc. Refrig. Air Condition. Eng, 2013, 30(3): 213-220.
[24] S. J. Kline, F. A. Mcclintock. Describing uncertainties in single-sample experiments[J]. Mechanical engineering, 1953, 75(1): 3-8.
[25] S. Sircar. Linear-driving-force model for non-isothermal gas adsorption kinetics[J]. Journal of the Chemical Society Faraday Transactions, 1983,79: 785-796.

[26] A. Chakraborty, B. Sun. An adsorption isotherm equation for multi-types adsorption with thermodynamic correctness[J]. Applied Thermal Engineering, 2014, 72(2): 190-199.
[27] J. M. Goldsworthy. Measurements of water vapour sorption isotherms for RD silica gel, AQSOA-Z01, AQSOA-Z02, AQSOA-Z05 and CECA zeolite 3A[J]. Microporous and Mesoporous Materials, 2014, 196: 59-67.
[28] L. Liu, T. Zeng, H. Huang, et al. Numerical modelling and parametric study of an air-cooled desiccant coated cross-flow heat exchanger[J]. Applied Thermal Engineering, 2020, 169: 114901.
[29] A. Entezari, T. S. Ge, R. Z. Wang. Water adsorption on the coated aluminum sheets by composite materials (LiCl + LiBr)/silica gel[J]. Energy, 2018, 160: 64-71.
[30] Z. Li, S. Michiyuki, F. Takeshi. Experimental study on heat and mass transfer characterisics for a desiccant-coated fin-tube heat exchanger[J]. International Journal of Heat and Mass Transfer, 2015, 89: 641-651.
[31] H. Heyden, G. Munz, L. Schnabel, et al. Kinetics of water adsorption in microporous aluminophosphate layers for regenerative heat exchangers[J]. Applied Thermal Engineering, 2009, 29(8-9): 1514-1522.
[32] A. Patton, B. D. Crittenden, S. P. Perera. Use of the Linear Driving Force Approximation to Guide the Design of Monolithic Adsorbents[J]. Chemical Engineering Research and Design, 2004, 82(8): 999-1009.
[33] H. W. B. Teo, A. Chakraborty, W. Fan. Improved adsorption characteristics data for AQSOA types zeolites and water systems under static and dynamic conditions[J]. Microporous and Mesoporous Materials, 2017, 242: 109-117.
[34] C. R. Ruivo, A. R. Figueiredo, J. J. Costa. Comparative assessment of the linear driving force and pseudo-gas-side-controlled models for the prediction of mass transfer in desiccant matrices[J]. Energy, 2014, 75: 603-612.